I&EC research
Industrial & Engineering Chemistry Research

Article

pubs.acs.org/IECR

Dominant Scaling Groups of Polymer Flooding for Enhanced Heavy Oil Recovery

Ziqiang Guo,[†] Mingzhe Dong,*[,†] Zhangxin Chen,[†] and Jun Yao[‡]

[†]Department of Chemical and Petroleum Engineering, University of Calgary, Calgary, Alberta, Canada T2N 1N4

[‡]College of Petroleum Engineering, China University of Petroleum (East), Qingdao, Shandong, China 266555

Supporting Information

ABSTRACT: Polymer flooding of heavy oils on the laboratory scale shows appreciable incremental tertiary oil recovery. In reality, however, this high recovery efficiency usually cannot be achieved in the field due mainly to extremely unfavorable mobility ratio and reservoir heterogeneity. The former promotes viscous fingering while the latter induces channeling; hence both of these factors make the displacement process less efficient. This paper identifies the dominant scaling groups for polymer flooding currently conducted in western Canadian heavy oil reservoirs. Twenty-eight dimensionless scaling groups governing the process of polymer flooding for enhanced heavy oil recovery were derived using inspectional analysis, and a fully tuned numerical model for polymer flooding of a heavy oil sample in a two-dimensional sand pack was then developed to validate the effectiveness of these scaling groups. A good agreement among different cases with the same group values was observed, showing the validity of the scaling groups. The effect of each scaling group on oil recovery was examined by numerical sensitivity analysis. By doing so, nine scaling groups dominating polymer flooding enhanced heavy oil recovery were identified. These dominant scaling groups can be used to design scaled experiments to predict field-scale oil recovery by polymer flooding in heavy oil reservoirs.

1. INTRODUCTION

With the decrease in conventional oil reserves and the ever-increasing oil price, heavy oil reserves have gained increasing attention as the next viable source of energy. Presently, thermal recovery methods are the most effective techniques for heavy oil production.[1] However, many heavy oil reservoirs in the world, such as heavy oil reservoirs located in western Canada, are housed in relatively thin pay zones which, owing to excessive heat losses to overburden and underburden formations, may render the application of thermal enhanced recovery technology uneconomical. It is generally accepted that heat losses in reservoirs with thicknesses less than 10 m would be very significant.[2] As for waterflooding of heavy oil reservoirs, severe viscous fingering leaves a substantial amount of oil unrecovered. This bypassed volume of oil is ideally the target of polymer flooding.

Meanwhile, the wide application of horizontal wells in heavy oil production and the high oil price make the process of polymer flooding technically feasible and economically affordable for heavy oil reservoirs. Laboratory studies show that, for heavy oils with viscosities ranging from 300 to 1600 mPa·s, polymer flooding has the potential to recover twice as much oil as can be obtained from waterflooding.[3] By conducting polymer flooding experiments in sand packs, Wang and Dong investigated the potential of polymer flooding for heavy oils.[4] Their experimental results showed that polymer flooding can improve the tertiary heavy oil recovery by as much as 20.9% original oil in place (OOIP) in uniform sand packs. Wang and Dong later examined the relationship between tertiary oil recovery by polymer flooding and the effective viscosity of polymer solution.[5] They found that, for heavy oils in the viscosity range 430−5500 mPa·s, there is a characteristic viscosity of the injected polymer solution that optimizes heavy oil production.

Laboratory experiments reveal a promising prospect for polymer flooding in heavy oil reservoirs. However, on a field scale, the performance of polymer flooding is regrettably low. There is no gainsaying the fact that polymer flooding in heavy oil reservoirs bears a higher investment risk than in conventional oil reservoirs. To reduce the risk, it is crucial to quantitatively estimate the recovery from this enhanced oil recovery (EOR) process before it is implemented in the oil field. One way to do this is to conduct reservoir simulation studies. Due to the lack of historical production data of previous polymer flooding with which to do history matching, the reliability of reservoir simulation models can be hardly guaranteed. An alternative to reservoir simulation is to carry out laboratory-scale experiments and then use scaling groups to evaluate field-scale performance. This methodology is known as scale-up, which is both effective and convenient.

Scale-up is the process of extrapolating results obtained from a small scale system (e.g., a laboratory core or sand pack) to a larger scale system (e.g., a well pattern unit or a reservoir). This process has been successfully used in chemical engineering (reactor design),[6,7] fluid mechanics (large shipbuilding),[8] and aerodynamics (wind tunnel experiments).[9] Laboratory sand packs are used, as is the tradition in the petroleum industry, to replicate the porous media of heavy oil reservoirs. Such replicas are then used in experiments to investigate the effectiveness of EOR processes before the processes are applied in the field. To facilitate the reliability of predictions from experiments and improve their applicability in the field, it is first necessary to establish a set of

Received: June 22, 2011
Revised: November 30, 2012
Accepted: December 12, 2012
Published: December 12, 2012

ACS Publications © 2012 American Chemical Society

dx.doi.org/10.1021/ie300328y | *Ind. Eng. Chem. Res.* 2013, 52, 911−921

relationships between the two systems, the sand pack and the reservoir. These relationships are known as scaling groups.

A scaling group is a combination of dimensional or dimensionless quantities such that the resultant possesses zero overall dimensions. Two methods are generally used to derive the dimensionless scaling groups: inspectional analysis[10] and dimensional analysis.[11] Inspectional analysis requires the exact equations governing a physical process, such as a fluid displacement process in a porous medium, whereas dimensional analysis only requires the knowledge of the pertinent variables affecting the displacement. In inspectional analysis, linear transformations are defined to convert every dimensional variable that appears in the differential equations governing the displacement into a dimensionless equivalent. On substituting all the transformations into the original equations, the dimensionless scaling groups can be obtained. In dimensionless analysis, however, there is no need to exactly know the equations describing the process. In order to obtain dimensionless scaling groups of the displacement, it is required that the power products of the variables be dimensionless. Each method has its own advantages and limitations. Inspectional analysis usually generates fewer scaling groups with apparent physical meanings, while dimensional analysis results in a large number of groups, some of which may have no physical interpretations.[12]

Scale-up studies of multiphase flow in porous medium have been extensively conducted in the past. Rapoport presented for the first time an inspectional analysis derivation to come up with a scaling relationship of immiscible displacement of oil by cold water.[13] His derivation was under the assumptions that the initial fluid distribution, the relative permeability functions, and the oil−water viscosity ratio must be the same for both the model and prototype. In addition, the author also pointed out that the application of the scaling laws requires the porous media to have different specific permeabilities and porosities but possess identical relative permeability curves. In most cases it may be impossible to find a suitable material for the construction of a model which permits quantitative scaling of the flow process in a given reservoir. Van Daalen and Van Domslaar made a scaling analysis for models with different geometries.[14] They found that the aspect ratio did not affect recovery of immiscible displacements if there is no cross-flow; otherwise, the aspect ratio becomes important in the scaling. Thomas et al. described scaling criteria for a micellar flooding process from the basic mass balance equations using both inspectional analysis and dimensional analysis.[15] Fifty-six groups from inspectional analysis and 71 from dimensional analysis were obtained. Micellar flooding experiments were carried out in sandstone cores of two different sizes, and the scaled-up recovery curves were compared with the predicted recovery curve. The agreement between the predicted and actual recoveries was good in some cases and poor in others. Scale-up of miscible flooding has been extensively studied by Gharbi et al.[16,17] They established the relationship between the fractional oil recovery and the dominant scaling groups in miscible displacement using artificial neural network models. Algharaib et al. made a scaling analysis for immiscible displacement with different configurations of horizontal wells and provided a quick prediction tool for the fractional oil recovery.[18] Jin et al. presented scaling groups specific for well production with a downhole water loop (DWL) system using inspectional analysis.[19] A total of four dimensionless groups were identified as the dominant factors describing the DWL system. In a recent study by Zendehboudi et al., dimensional analysis was conducted to investigate the controlled gravity drainage (CGD) process in a fractured porous medium and a prediction model was developed and verified to estimate the critical operational parameters of oil production under CGD in fractured reservoirs.[20] Most of the previous scale-up studies were focused on developing scaling groups for waterflooding or miscible flooding. There are very few studies regarding the scale-up of polymer flooding. A set of scaling criteria were developed for polymer, emulsion, and foam flooding by Islam and Farouq Ali.[21] They recommended key scaling groups of polymer flooding for different scenarios by qualitative analysis. The effectiveness of their scaling groups was not validated, and the effect of each scaling group on oil recovery was not examined either. Rai[22] derived dimensionless groups for surfactant−polymer flooding and validated the groups. Sensitivity tests were carried out for each group to study their relative importance on recovery performance. In each test, the group under study was varied while the rest of the groups were held constant. Scaling groups having minimal effect on oil recovery were relaxed from the scaling. However, the effects of polymer adsorption, inaccessible pore volume, and permeability reduction were not included. To the best knowledge of the authors, no scale-up study for polymer flooding of heavy oils exists in the literature.

The objective of this study is to present a set of dominant scaling groups for polymer flooding in heavy oil reservoirs, based on which scaled laboratory experiments can be designed to predict field-scale heavy oil recovery. First, the mathematical model of polymer flooding of heavy oils is set up, together with a brief review of the mechanisms that interplay in the process. Since the underlying physical laws governing the flooding process are readily known, inspectional analysis is chosen over dimensional analysis to derive the scaling groups for the process. In the second step, by history matching experimental results of polymer flooding of a heavy oil sample, a fully tuned numerical model is obtained and used to examine the effectiveness of these scaling groups. Finally, numerical methods are used to investigate the sensitivity of heavy oil recovery to each scaling group; groups with less influence are relaxed to reduce the number of scaling groups. Subsequently, nine dominant groups are obtained; they can be used to design scaled laboratory experiments to predict heavy oil recovery by polymer flooding.

2. GOVERNING EQUATIONS OF POLYMER FLOODING FOR HEAVY OILS

The governing equations were written under the following assumptions:

1. The polymer flooding process involves only two phase flows: oleic phase and aqueous phase. Polymer is only present in the aqueous phase.
2. Rock and fluids are incompressible and the dispersion of polymer is negligible.
3. The injected polymer only reduces the permeability of the aqueous phase and has no effect on that of oleic phase.
4. In situ water, makeup water for polymer solution, and drive water all have the same physical properties.

The two-dimensional (x,z) model[16] used for the derivation of the dimensionless scaling groups is shown is Figure 1. The process of polymer flooding of heavy oils in this two-dimensional (2-D) model is governed by the following conservation equations, continuity equations, constitutive equations, and equations describing the properties of the polymer solution.

2.1. Flooding Process Related Equations. Typical polymer flooding involves three consecutive injection processes: initial waterflooding, polymer slug injection, and extended waterflooding. After injecting a certain amount (PV_{w1}) of water, a polymer slug of size PV_p is injected and followed by extended water (PV_{w2}).

dx.doi.org/10.1021/ie300328y | Ind. Eng. Chem. Res. 2013, 52, 911−921

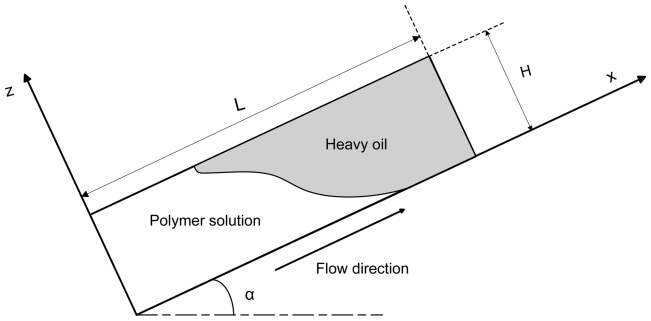

Figure 1. Displacement of heavy oils by polymer solution in a 2-D porous medium.

The conservation equation for the oleic phase is

$$\phi \frac{\partial S_o}{\partial t} + \frac{\partial V_{ox}}{\partial x} + \frac{\partial V_{oz}}{\partial z} = 0 \tag{1}$$

where ϕ is the porosity, S_o is the oil saturation, t is time, and V_{ox} and V_{oz} are the velocities of oil flow in the x-direction and z-direction, respectively.

The conservation equation for the aqueous phase is given by

$$\phi \frac{\partial S_a}{\partial t} + \frac{\partial V_{ax}}{\partial x} + \frac{\partial V_{az}}{\partial z} = 0 \tag{2}$$

where S_a is the saturation of the aqueous phase and V_{ax} and V_{az} are the velocities of the aqueous phase flow in the x-direction and z-direction, respectively.

The saturations of the oleic and aqueous phases are such that

$$S_o + S_a = 1 \tag{3}$$

Combining eqs 1−3 shows that

$$\frac{\partial(V_{ox} + V_{ax})}{\partial x} + \frac{\partial(V_{oz} + V_{az})}{\partial z} = 0 \tag{4}$$

Equations 1−4 are used for all three injection stages.

There is a unique equation for the polymer slug injection. The mass balance equation for polymer is written as

$$(\phi - \phi_{IPV}) \frac{\partial(S_a C_{pa})}{\partial t} + \phi \frac{\partial(C_{ad})}{\partial t} + \frac{\partial(C_{pa} V_{ax})}{\partial x} + \frac{\partial(C_{pa} V_{az})}{\partial z} = 0 \tag{5}$$

where ϕ_{IPV} is the polymer inaccessible porosity, C_{pa} is the polymer concentration in aqueous phase, and C_{ad} is the polymer adsorption concentration.

The continuity equations for waterflooding are as follows:

$$V_{ax} = -\frac{k_x}{\mu_a R_k} k_{ra} \left(\frac{\partial P_a}{\partial x} + \rho_a g \sin \alpha \right) \tag{6}$$

$$V_{ox} = -\frac{k_x}{\mu_o} k_{ro} \left(\frac{\partial P_o}{\partial x} + \rho_o g \sin \alpha \right) \tag{7}$$

$$V_{az} = -\frac{k_z}{\mu_a R_k} k_{ra} \left(\frac{\partial P_a}{\partial z} + \rho_a g \cos \alpha \right) \tag{8}$$

$$V_{oz} = -\frac{k_z}{\mu_o} k_{ro} \left(\frac{\partial P_o}{\partial z} + \rho_o g \cos \alpha \right) \tag{9}$$

where, respectively, k_x and k_z are the absolute permeabilities in the x-direction and the z-direction, μ_a is the viscosity of the aqueous phase, μ_o is the oil viscosity, P_a and P_o are the aqueous phase pressure and oleic phase pressure, ρ_a and ρ_o are the aqueous phase density and oleic phase density, g is the gravitational acceleration, α is the dip angle of the model with respect to the horizontal, R_k is the permeability reduction factor to the aqueous phase, and, for waterflooding $R_k = 1$, k_{ra} and k_{ro} are the respective relative permeabilities to the aqueous phase and the oleic phase, which can be written as[23]

$$k_{rl} = k_{rl}^0 (S_{nl})^{n_l} \qquad \text{for } l = \text{a, o} \tag{10}$$

where k_{rl}^0 is the end point relative permeability to phase l, n_l is the relative permeability exponent for phase l, and S_{nl} is the normalized saturation for phase l defined as

$$S_{nl} = \frac{S_l - S_{lr}}{1 - S_{wr} - S_{or}} \qquad \text{for } l = \text{a, o} \tag{11}$$

where S_{wr} is the irreducible aqueous phase saturation and S_{or} is the residual oil saturation.

The pressure in the oleic phase and that in the aqueous phase are related by[19]

$$P_o = P_a + P_c = P_a + P_{ce} S_{na}^{-1/\lambda_i} \tag{12}$$

where P_c is the capillary pressure between the phases, P_{ce} is the entry capillary pressure of the rock sample, and λ_i is the pore size distribution index.

Initial conditions are

$$S_a = S_{wi}, \qquad \text{at} \qquad t = 0, \ \forall\, x, z \tag{13}$$

where S_{wi} is the initial water saturation.

For polymer injection, there is an additional initial condition:

$$C_{pa} = 0, \qquad \text{at} \qquad t = 0, \ \forall\, x, z \tag{14}$$

Boundary conditions are

$$V_{az} = 0, \qquad \text{at} \qquad z = 0, \ \forall\, x, t \tag{15}$$

$$V_{az} = 0, \qquad \text{at} \qquad z = H, \ \forall\, x, t \tag{16}$$

$$V_{oz} = 0, \qquad \text{at} \qquad z = 0, \ \forall\, x, t \tag{17}$$

$$V_{oz} = 0, \qquad \text{at} \qquad z = H, \ \forall\, x, t \tag{18}$$

$$S_a = 1 - S_{or}, \qquad \text{at} \qquad x = 0, \ \forall\, z, t > 0 \tag{19}$$

$$C_{pa} = C_{pa}^i, \qquad \text{at} \qquad x = 0, \ \forall\, z, t \tag{20}$$

where H is the linear dimension of the model in the z-direction and C_{pa}^i is the concentration of the injected polymer solution. Equation 20 is the boundary condition only for polymer slug injection.

The injector equation is

$$\frac{1}{H} \int_0^H V_{ax}\, dz = V_T, \qquad \text{at} \qquad x = 0, \ \forall\, t \tag{21}$$

where V_T is the average total velocity.

The producer equation is

$$P_a = P_{wf} + \rho_{avg} g \cos \alpha (H - z) \qquad \text{at} \qquad x = L, \ \forall\, z, t \tag{22}$$

$$P_o = P_{wf} + \rho_{avg} g \cos \alpha (H - z) \qquad \text{at} \qquad x = L, \ \forall\, z, t \tag{23}$$

dx.doi.org/10.1021/ie300328y | Ind. Eng. Chem. Res. 2013, 52, 911−921

Table 1. Dimensionless Scaling Groups Governing the Process of Polymer Flooding[a]

i	1	2	3	4	5	6	7	8	9
D_i	ϕ	S_{wr}	S_{or}	n_a	k_z/k_x	n_o	$\frac{\mu_w k_{ro}^0}{\mu_o k_{ra}^0}$	ρ_o/ρ_w	$\frac{k_{ro}^0 k_z \rho_o g \cos\alpha}{V_T \mu_o}$
i	10	11	12	13	14	15	16	17	18
D_i	$\tan\alpha$	L/H	$\frac{k_{ro}^0 k_x P_{ce}}{\mu_o L V_T}$	S_{wi}	ϕ_{IPV}	$R_{k,max}$	$b_{rk}C_{pa}^i$	$A_{p1}C_{pa}^i$	$A_{p2}C_{pa}^{i\,2}$
i	19	20	21	22	23	24	25	26	27	28
D_i	$A_{p3}C_{pa}^{i\,3}$	$\frac{CV_T}{\gamma_{1/2}\sqrt{k_x k_{ra}^0}}$	P_α	$\frac{C_{ad,max}}{C_{pa}^i}$	bC_{pa}^i	PV_{wl}	PV_p	PV_{w2}	V_{DP}	λ_L

[a]The physical meaning of each scaling group is discussed as follows: D_1 = porosity of 2-D model; D_2 and D_3 = irreducible water saturation and residual oil saturation, respectively; D_4 and D_6 = relative permeability exponents for aqueous phase and oleic phase, respectively; D_5 = ratio of vertical permeability to horizontal permeability of 2-D model; D_7 = end point mobility ratio of oleic phase to water phase; D_8 = ratio of oil density to water density; D_9 = ratio of gravity force to viscous pressure drop; D_{10} = tangent of the dip angle of the 2-D model; D_{11} = aspect ratio of the 2-D model, i.e., ratio of length to width of the model; D_{12} = ratio of capillary force to viscous pressure drop; D_{13} = initial water saturation; D_{14} = porosity that is inaccessible to polymer solution; D_{15} = maximum permeability reduction factor for aqueous phase; D_{16} = parameter related to permeability reduction ability of polymer solution; D_{17}, D_{18}, and D_{19} = dimensionless coefficients in eq 25 for calculation of the viscosity of polymer solution as a function of polymer concentrations at zero shear rate; D_{20} = ratio of viscous force to shear thinning force; D_{21} = empirical exponent that describes the shear thinning effect; D_{22} = ratio of maximum polymer adsorption concentration to initial polymer concentration; D_{23} = rock characteristics related to adsorption behavior; D_{24}, D_{25}, and D_{26} = slug sizes for initial waterflooding, polymer flooding, and extended waterflooding, respectively; D_{27} = Dykstra–Parson coefficient; D_{28} = dimensionless correlation in the displacement direction.

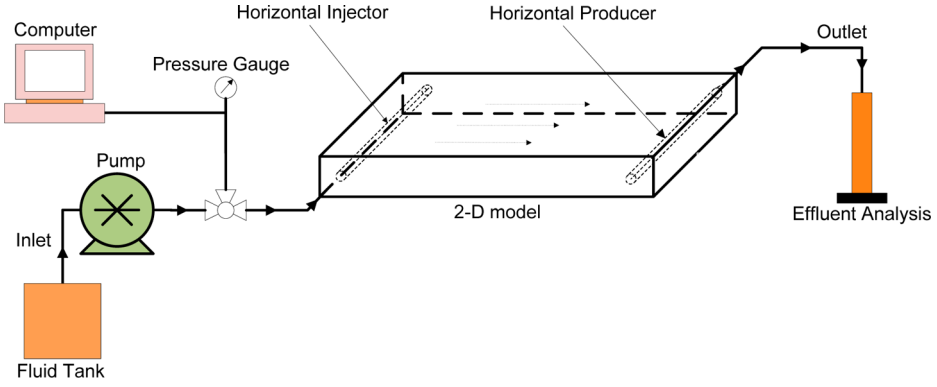

Figure 2. Schematic of 2-D sand-pack polymer flooding with effluents measured at ambient.

where P_{wf} is the well flowing pressure at $(x, z) = (L, H)$, L is the length of the model in the x-direction, and ρ_{avg} is the average density, which is calculated as

$$\rho_{avg} = \rho_o + (\rho_a - \rho_o)\frac{\int_0^H V_{ax}\,dz}{HV_T} \qquad \text{at} \qquad x = L,\ \forall\, t \tag{24}$$

2.2. Polymer Solution Property Equations. The viscosity of the polymer solution under the zero shear rate μ_p^0 is given by Flory[24] as

$$\mu_p^0 = \mu_w(1 + (A_{p1}C_{pa} + A_{p2}C_{pa}^{\ 2} + A_{p3}C_{pa}^{\ 3})C_{SEP}^{\ S_p}) \tag{25}$$

where μ_w is the water viscosity, A_{p1}, A_{p2}, and A_{p3} are parameters used for calculating the polymer viscosity at zero shear, C_{SEP} is the effective salinity, and S_p is the slope of $(\mu_p^0 - \mu_w)/\mu_w$ vs C_{SEP} on a log–log plot. In this study, the salinity effect is neglected by setting $S_p = 0$.

The reduction in the viscosity of the polymer solution as a function of the shear rate γ is modeled by Meter's equation:[25]

$$\mu_p = \mu_w + \frac{\mu_p^0 - \mu_w}{1 + \left(\frac{\gamma}{\gamma_{1/2}}\right)^{P_\alpha - 1}} \tag{26}$$

where μ_p is the effective viscosity of the polymer solution, γ is the shear rate, $\gamma_{1/2}$ is the shear rate at which the viscosity is the average of μ_p^0 and μ_w, and P_α is an empirical shear thinning coefficient.

For multiphase flow in porous media, μ_p is usually referred to as the apparent viscosity and the in situ shear rate for phase l is usually calculated by the modified Blake–Kozeny capillary bundle equation for multiphase flow as[26]

$$\gamma = \frac{3.97C\sqrt{V_{ax}^{\ 2} + V_{az}^{\ 2}}}{\sqrt{\bar{k}k_{ra}\phi S_a}} \tag{27}$$

where C is the shear rate coefficient used to account for nonideal effects such as slip at the pore walls,[27] and $\bar{k}$ is the average permeability, which can be expressed as

$$\bar{k} = \left(\frac{1}{k_x}\frac{V_{ax}^{\ 2}}{V_{ax}^{\ 2} + V_{az}^{\ 2}} + \frac{1}{k_z}\frac{V_{az}^{\ 2}}{V_{ax}^{\ 2} + V_{az}^{\ 2}}\right)^{-1} \tag{28}$$

For a given porous medium, polymer adsorption can be described by a Langmuir-type isotherm given by[28]

dx.doi.org/10.1021/ie300328y | Ind. Eng. Chem. Res. 2013, 52, 911–921

Table 2. Parameters Adjusted To Match Experimental Results of Polymer Flooding for Brintnell Heavy Oil

parameter	value	unit
k^0_{ra}	0.4	
k^0_{ro}	1	
n_a	1.7	
n_o	1	
$C_{ad,max}$	0.02	mg/g
b	100	$(wt\ \%)^{-1}$
ϕ_{IPV}	0.1	

$$C_{ad} = C_{ad,max}\frac{bC_{pa}}{1 + bC_{pa}} \tag{29}$$

where $C_{ad,max}$ is the maximum polymer adsorption concentration and b controls the curvature of the isotherm.

A polymer solution can also reduce the effective permeability of the porous media by a factor of R_k:[29]

$$R_k = 1 + (R_{k,max} - 1)\frac{b_{rk}C_{pa}}{1 + b_{rk}C_{pa}} \tag{30}$$

where $R_{k,max}$ is the maximum permeability reduction factor, and b_{rk} is the parameter for calculation of permeability reduction factor.

Equations 25−30 are only for polymer slug injection.

3. DERIVATION OF SCALING GROUPS FOR POLYMER FLOODING

Linear transformations, with which to convert dimensional variables into their dimensionless equivalents, are defined as[30]

$$M = M_1^* M_D + M_2^* \tag{31}$$

where M denotes all the dimensional variables that appear in eqs 1−30, M_D is the dimensionless equivalent, and M_1^* and M_2^* are the multiplicative and the additive scale factors, respectively.

By applying all the transformations to eqs 1−30 in the inspectional analysis, 29 scaling groups were derived. Among them, 20 scaling groups were linearly independent and 9 were linearly dependent. These 9 groups contained 14 associated variables. The linear dependence between these nine groups was examined by evaluating the rank of the 9×14 nonsquare coefficient matrix. The rank of the matrix was determined to be 6 and three dependent groups were ruled out. Therefore, 26 linearly independent groups represented the minimum number of scaling groups describing the displacement.

These dimensionless scaling groups are actually the coefficients that appear in the dimensionless forms of eqs 1−30. Keeping the value of each of these scaling groups constant in any two dimensionally different systems (e.g., a sand pack and a reservoir) and solving the equations involved will yield identical solutions of the unknowns, regardless of the dimensional scale of the systems. Therefore, these scaling groups can be used to design scaled laboratory experiments from which field-scale recovery of heavy oils by polymer flooding can be predicted.

4. SCALING GROUPS FOR RESERVOIR HETEROGENEITY

Reservoir heterogeneity plays a critical role in determining the recovery from petroleum reservoirs. The sands of Canada's heavy oil reservoirs exhibit considerable heterogeneity,[31] which must be considered when designing parameters for field development using polymer flooding. In this study, log-normal distributed permeability fields were generated by unconditional sequential Gaussian simulation (SGSIM).[32] The measure of heterogeneity is completely described by the Dykstra−Parson coefficient V_{DP} and correlation length λ_L.[33]

The Dykstra−Parson coefficient, a measure of the permeability variation, has values of 0 for homogeneous and 1 for extremely heterogeneous. For real reservoirs, V_{DP} values estimated from well logs range from 0.65 to 0.99.[34] For a log-normal permeability distribution, V_{DP} is calculated as[35]

$$V_{DP} = 1 - \exp(-\sigma_{\ln k}) \tag{32}$$

where $\sigma_{\ln k}$ is the standard deviation of the log values of permeabilities.

λ_L determines how well neighboring permeability values are related to each other,[33] which is defined as a fraction of the reservoir length in the longitudinal flow direction. When λ_L is small, there is little correlation between neighbors; as λ_L approaches infinity, the reservoir becomes strictly layered.

Combining the 26 groups derived in section 3, there are a total of 28 scaling groups that govern the process of heavy oil recovery by polymer flooding, as listed in Table 1.

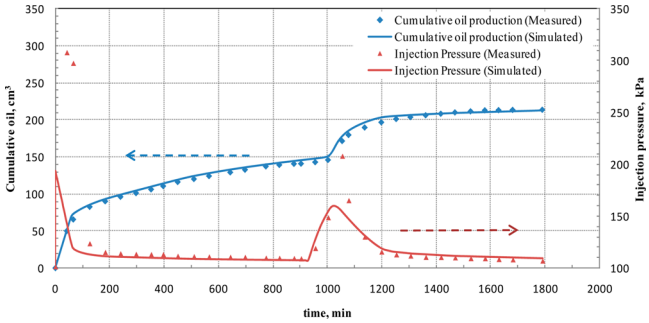

Figure 3. Measured and simulated cumulative oil production and injection well pressure.

Table 3. Parameters Involved in Scaling Groups

	case 1	case 2	case 3	case 4	case 5
L (m)	0.5	5	0.5	0.5	500
H (m)	0.2	2	0.2	0.2	200
α (deg)	30	30	30	30	30
k_z (μm^2)	2	2	1	4	4
k_x (μm^2)	5	5	2.5	10	10
μ_w (mPa·s)	1	1	0.5	1	1
μ_o (mPa·s)	1000	1000	250	1000	2400
ρ_o (kg/m^3)	900	900	900	900	900
ρ_w (kg/m^3)	1000	1000	1000	1000	1000
k^0_{ra}	0.4	0.4	0.4	0.2	0.1
k^0_{ro}	1	1	0.5	0.5	0.6
q (m^3/day)	0.0005	0.005	0.0005	0.0005	0.25
P_{ce} (kPa)	5	50	3.54	7.077	7071.07
C^i_{pa} (wt %)	0.1	0.15	0.2	0.25	0.3
b $(wt\ \%)^{-1}$	100	66.67	50	40	33.337
b_{rk} $(wt\ \%)^{-1}$	1	0.67	0.5	0.4	0.33
A_{p1} $(wt\ \%)^{-1}$	80	53.33	40	32	26.67
A_{p2} $(wt\ \%)^{-2}$	1600	711.11	400	256	177.78
A_{p3} $(wt\ \%)^{-3}$	10000	2962.96	1250	640	370.37
C (s^{-1})	4	4	2.83	4	4
$\gamma_{1/2}$ (s^{-1})	20	20	20	20	14.14
V_{DP}	0.1	0.1	0.1	0.1	0.1
λ_L	0.1	0.1	0.1	0.1	0.1

dx.doi.org/10.1021/ie300328y | Ind. Eng. Chem. Res. 2013, 52, 911−921

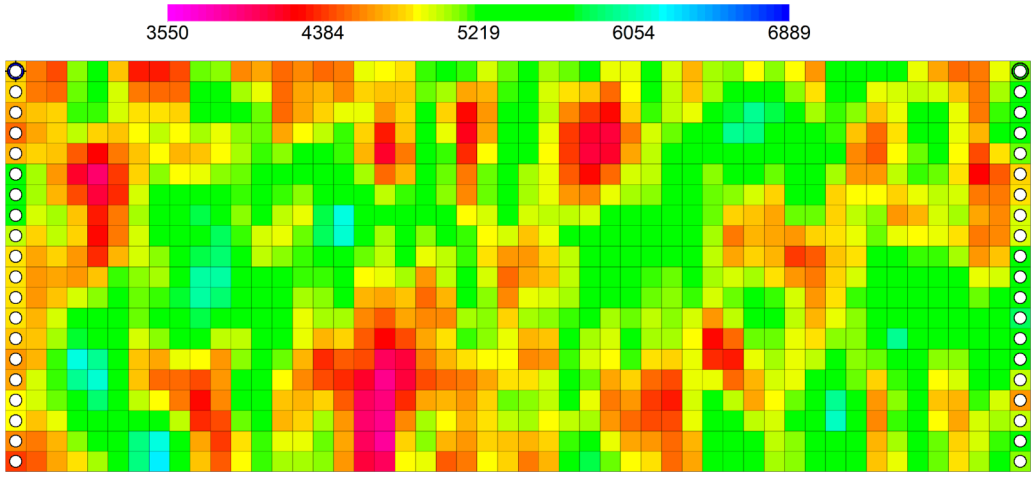

Figure 4. Heterogeneous permeability distribution generated using SGSIM.

Table 4. Identical Group Values for Five Cases

i	1	2	3	4	5	6	7	8	9
D_i	0.4	0.07	0.3	1.7	0.4	1	0.0025	0.9	4.15×10^{-8}
i	10	11	12	13	14	15	16	17	18
D_i	0.58	2.5	0.0566	0.07	0.1	10	0.1	8	16
i	19	20	21	22	23	24	25	26	27	28
D_i	10	3.54×10^4	1.1	0.2	10	3	0.6	2.45	0.1	0.1

5. VALIDATION OF SCALING GROUPS

A total of 28 dimensionless scaling groups have been defined above. To validate the effectiveness of these scaling groups, fine-mesh numerical simulations are performed. First, a fully tuned numerical model is developed by history matching the experimental results of polymer flooding of a heavy oil sample. Then five simulation runs, with the same scaling group values but with different combinations of physical parameters, are conducted. The oil recovery performances of the five runs are then compared. Achieving the identical level of recovery in all the runs ultimately will suggest that the dimensionless scaling groups are effective.

5.1. History Match of Experimental Results. A 2-D sand-pack (see Figure 2) polymer flooding test for heavy oil production was conducted at ambient temperature (22 °C). The figure shows two horizontal wells that transverse the length of the model, one of which is an injector and the other is a producer. A heavy oil sample, Brintnell heavy oil, from western Canadian heavy oil reservoirs with a viscosity of 1020 mPa·s at 22 °C, was used in this study. AN923PGO polymer of concentration 1000 ppm (0.1 wt %), provided by SNF Floerger (France), was used in the flooding test. The polymer flooding test was preceded by a waterflooding and then followed by an extended waterflooding.

A $50 \times 20 \times 1$ grid system is used to history match the polymer flooding test in a $9 \times 6 \times 1$ in. sand pack. First of all, a history match of the initial waterflooding furnishes the set of relative permeability curves used in the subsequent tests. The following polymer flooding is then matched to obtain the polymer adsorption data and the inaccessible pore volume. A tabulation of the values of the history-matched parameters is shown in Table 2. The history-matched cumulative oil production and injection pressure are shown in Figure 3.

5.2. Validation of the Scaling Groups. After setting up the simulation model, five simulation cases are run with the same group values but with different combinations of parameters. All the runs are conducted with the chemical flooding simulation software UTCHEM. The individual parameters involved in scaling groups are shown in Table 3. The group values calculated from these parameters are the same among the five cases. For the heterogeneity scaling groups, $V_{DP} = 0.1$ and $\lambda_L = 0.1$ are used to generate the permeability field, as shown in Figure 4. The identical group values for the five cases are presented in Table 4.

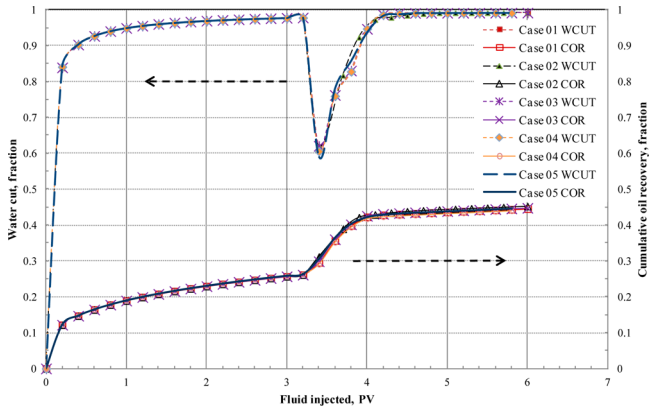

Figure 5. Comparison of cumulative oil recovery (COR) and water cut (WCUT) for the five cases.

Figure 5 shows the comparison of cumulative oil recovery and water cut for the five cases. For the waterflooding part, the oil recovery curves for these five cases are matched very well; for the polymer flooding part, the difference in oil recovery is within 1%. Essentially, there is good agreement in all five cases, which strongly indicates the validity of the scaling groups.

Figure 6 shows the water saturation distribution at the end of the polymer flooding for each of the five cases. The water distribution is almost the same for all the cases, suggesting that the 28 scaling groups identified in this study govern polymer flooding for heavy oil recovery.

dx.doi.org/10.1021/ie300328y | Ind. Eng. Chem. Res. 2013, 52, 911−921

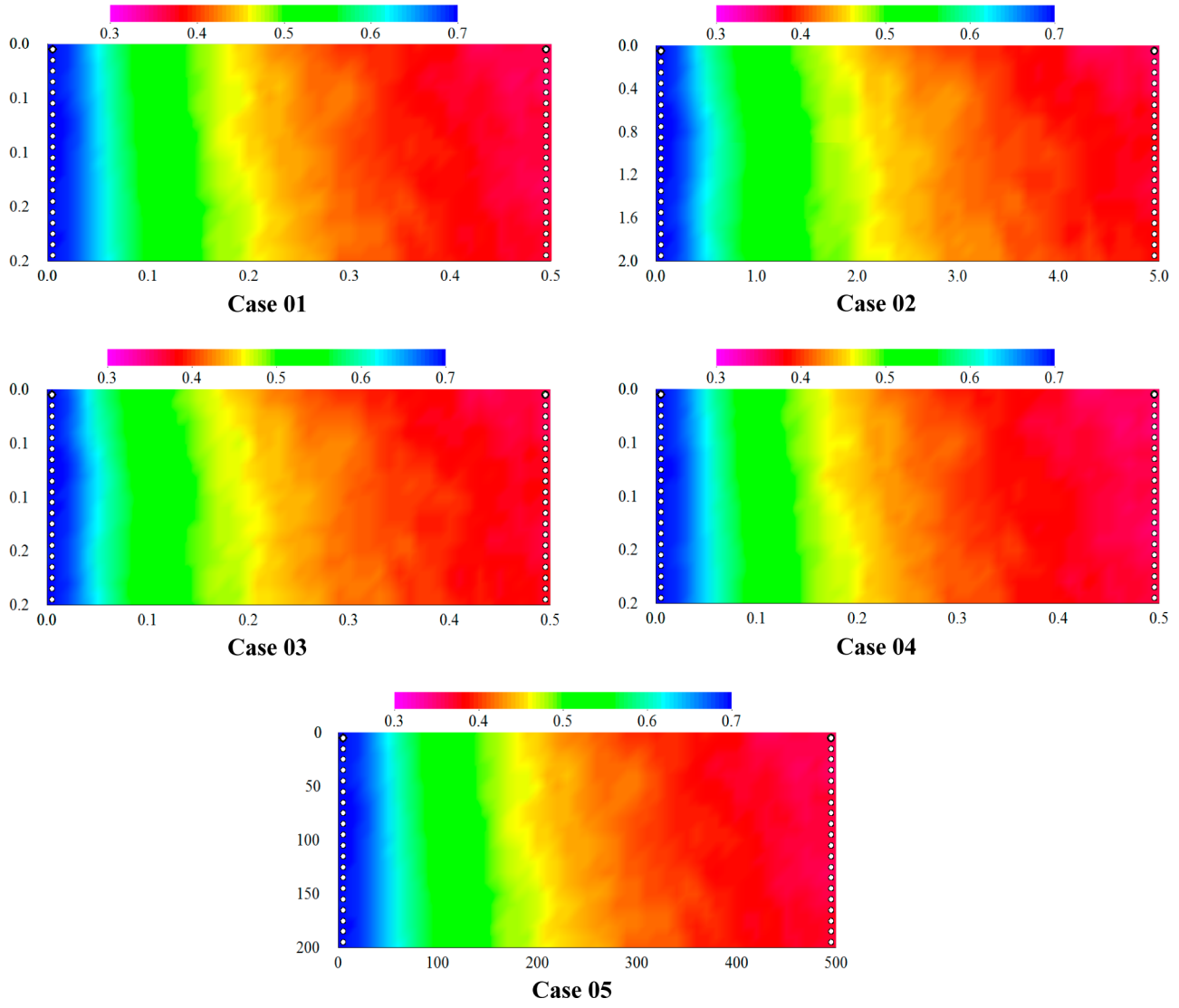

Figure 6. Water saturation distribution after an injection of 6.05 PV fluids.

6. DOMINANT SCALING GROUPS FOR POLYMER FLOODING OF HEAVY OILS

Twenty-eight dimensionless scaling groups have been obtained in this study. It is often very difficult, if not impossible, to keep the values of all these groups in laboratory experiments identical to those in the field. For instance, in order to keep the values of all scaling groups the same among the above five cases, the entry capillary pressure of rock sample P_{ce} in case 5 has to be set to a unrealistically large value (7071.07 kPa). Hence, in conducting experiments, it is of critical importance to identify the dominant (or primary) dimensionless groups and relax the less dominant (or secondary) ones.

6.1. Numerical Sensitivity Analysis. Due to excessive workload and great demand on resources, it may be unrealistic to design laboratory experiments for the evaluation of the effect of each scaling group on oil recovery. In this study, numerical experiments were conducted to determine the impact of each scaling group. For all the experiments, the permeability reduction factor was changed by varying $b_{rk}C^{i}_{pa}$ while keeping $R_{k,max}$ at a constant level. The effects of initial (PV_{w1}) and extended waterflooding (PV_{w2}) are not the scope of this study. Therefore, in each experiment 3 pore volumes (PV) of water was injected prior to polymer slug (PV_p) injection and the total injected fluid was fixed at 4.6 PV. Therefore, the effects of groups 15, 24, and 26 were not examined in this study.

Since the sensitivity analysis involves 25 groups, a complete factorial design is not acceptable. For instance, a simple two-level design would generate 2^{25} ($\approx 3.4 \times 10^8$) experiments. When there are too many factors, a well-known experimental design method, the Plackett–Burman method (PB),[36] can be used as a screen to identify the most important ones. The PB design requires two levels (high and low) for each factor, which are given in Table 5. A 36-run PB design was used to study the effects of 25 factors on heavy oil recovery. The combinations of the group levels to be used in each run are shown in Table 7 in the Appendix.

After running the numerical experiments, statistical tests with a significance level (α) of 0.05 were used to analyze the results of 36 numerical experiments. For each scaling group, a standardized effect (t statistics) was calculated by dividing each regression coefficient by its standard error. Figure 7 shows the normal plot of the standardized effect of each scaling group on heavy oil recovery. The vertical axis is the cumulative probability density function, and the horizontal axis represents the standardized effect. The blue line is an imaginary reference line corresponding

dx.doi.org/10.1021/ie300328y | Ind. Eng. Chem. Res. 2013, 52, 911−921

Table 5. Values of Each Group Corresponding to the Low and High Levels

D_i	low	high
1	0.2	0.4
2	0.035	0.07
3	0.15	0.3
4	1.7	3.4
5	0.1	0.4
6	1	2
7	0.00067	0.0067
8	0.9	1.1
9	2×10^{-8}	2×10^{-7}
10	0.09	0.58
11	0.1	5
12	0.00566	0.0566
13	0.07	0.3
14	0.02	0.1
16	0.1	0.5
17	4	8
18	8	16
19	5	10
20	57 700	200 000
21	1.1	2.2
22	0.02	0.04
23	10	20
25	0.3	0.6
27	0.1	0.9
28	0.1	2

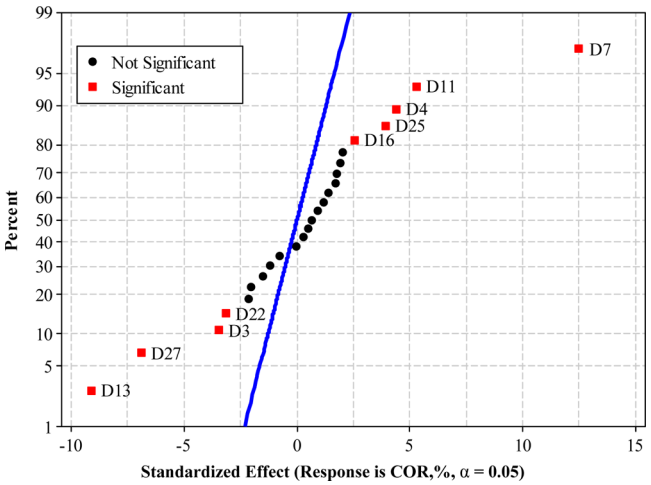

Figure 7. Normal plots of standardized effect of each scaling group.

to $\alpha = 0.05$. Plotted points falling far away from the imaginary line, upper right and lower left corners of the plot (Figure 7), indicate estimated effects that may be statistically significant.[37] The upper right points suggest a positive effect on heavy oil recovery, while the lower left ones indicate a negative impact.

Figure 8 shows the magnitude and relative importance of each scaling group on heavy oil recovery. The red line corresponds to $\alpha = 0.05$, and the scaling groups having absolute values of standardized effects beyond the red line are considered as significant factors in the determination of heavy oil recovery.

As can be seen from Figures 7 and 8, the most important groups affecting the heavy oil recovery are groups 7, 13, 27, 11, 4, 25, 3, 22, and 16. They are listed in Table 6.

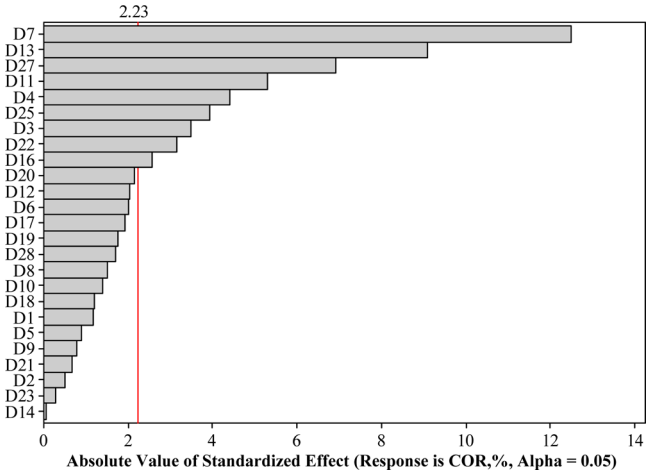

Figure 8. Pareto chart indicating the significance of each group in the determination of heavy oil recovery.

The above nine scaling groups can be used as major criteria in the design of scaled laboratory experiments and prediction of field-scale heavy oil recovery by polymer flooding.

6.2. Discussion. *6.2.1. Dominant Scaling Groups.* Scaling group 7, the end-point mobility ratio of oleic phase to water phase, has the largest effect on enhanced heavy oil recovery by polymer flooding. In heavy oil reservoirs, the poor mobility ratio is the main cause for oil bypassing and residual oil at the end of the displacement. Increasing the mobility ratio can improve the heavy oil flow capability and increase the displacement efficiency. According to the expression of scaling group 7, the mobility ratio can be increased by either increasing the viscosity of the aqueous phase (adding polymer) or reducing the oleic phase viscosity by thermal injection.

Group 13 is the initial water saturation, and it has a significant effect on heavy oil recovery. An increase in S_{wi} will increase the thickness of wetting layers and result in more snap-off and oil trapping.

Group 27 is the Dykstra–Parson coefficient V_{DP}, and it measures the variability of permeability distribution. As V_{DP} increases, injected water and polymer tend to channel through the high permeable zones and bypass a large amount of heavy oil in the low permeable zones.

The aspect ratio, group 11, also greatly affects the enhanced heavy oil recovery by polymer flooding. When the aspect ratio is small, the injected fluid quickly breaks through to the production well through the high permeable zones. The succeeding injected fluid will preferentially flow through these low resistance water paths, resulting in a poor sweep efficiency. When the aspect ratio is large, water will gradually cross-flow to the low permeable zones through capillary imbibition and improve the sweep efficiency.

Group 4 is the relative permeability exponents for the aqueous phase in the Brooks–Corey relative permeability correlation.[14] It can greatly influence the flow capability of water and thus the heavy oil recovery.

Scaling group 25 is the injected pore volume of polymer solution. A larger slug of polymer solution means more heavy oil recovery. Considering the economic effect, there should be an optimum slug size for polymer solution.

Scaling group 3 is the residual oil saturation. It is related to displacement efficiency and can directly affect heavy oil recovery. However, its effect on heavy oil recovery is not as predominant as the mobility-related factors. Hence the most important

dx.doi.org/10.1021/ie300328y | Ind. Eng. Chem. Res. 2013, 52, 911–921

Table 6. Dominant Scaling Groups

i	7	13	27	11	4	25	3	22	16
D_i	$\frac{\mu_w k^0_{ro}}{\mu_o k^0_{ra}}$	S_{wi}	V_{DP}	L/H	n_a	PV_p	S_{or}	$\frac{C_{ad,max}}{C^i_{pa}}$	$b_{rk}C^i_{pa}$

Table 7. Plackett–Burman Design[a]

	D_i																								
std order	1	2	3	4	5	6	7	8	9	10	11	12	13	14	16	17	18	19	20	21	22	23	25	27	28
19	−	+	+	+	−	+	+	+	+	+	−	−	−	+	+	−	+	−	−	+	−	−	+	+	−
30	+	−	+	−	+	−	−	−	+	+	−	−	+	+	−	+	+	+	+	+	−	−	−	+	+
12	+	+	+	−	−	−	+	+	+	−	+	−	−	+	−	+	+	−	+	−	+	−	−	−	−
21	+	−	−	+	+	+	−	+	+	+	+	+	−	−	+	+	+	−	+	−	−	+	−	−	+
4	+	−	+	−	−	+	−	−	+	+	−	+	−	+	−	−	−	+	−	−	+	+	+	−	+
3	−	+	−	−	+	−	−	+	+	−	+	−	+	−	−	−	+	−	−	+	+	+	−	+	+
29	−	+	−	+	−	−	−	−	+	−	−	+	+	+	+	+	+	+	+	−	−	−	+	+	+
5	+	+	−	+	−	−	+	−	+	+	+	−	+	−	−	−	−	−	+	−	−	+	+	+	−
32	−	+	+	−	+	−	+	−	+	−	−	+	−	−	+	+	−	+	+	+	+	+	−	−	−
6	+	+	+	−	+	−	−	+	+	−	+	+	−	+	+	−	−	−	−	+	−	−	+	+	+
9	−	−	−	+	+	+	−	+	+	−	+	−	−	+	−	+	−	+	−	−	−	−	+	−	−
31	+	+	−	+	−	+	−	−	+	−	+	−	−	+	+	−	+	+	+	+	+	−	−	−	+
27	−	+	−	−	−	−	+	−	+	+	+	+	−	+	+	+	+	−	−	−	+	+	+	−	+
10	+	−	−	−	+	+	+	−	+	−	−	+	−	−	+	−	+	−	+	−	−	−	−	+	−
26	+	−	−	−	−	+	−	−	+	+	+	−	+	+	+	+	−	−	−	+	+	+	−	+	−
25	−	−	−	−	+	−	−	+	+	+	−	+	+	+	+	−	−	−	+	+	+	−	+	−	−
1	−	−	+	−	−	+	+	−	+	−	+	−	−	−	+	−	−	+	+	+	−	+	+	+	+
18	+	+	+	−	+	+	+	+	+	−	−	−	+	+	−	+	−	−	+	−	−	+	+	−	+
23	−	−	+	−	−	+	+	+	+	+	+	+	+	+	−	−	+	+	+	−	+	−	−	+	−
2	+	−	−	+	−	−	+	+	+	+	−	+	−	−	−	+	−	−	+	+	+	−	+	+	+
16	+	−	+	+	+	+	+	−	+	−	+	+	+	−	−	−	+	−	−	+	+	−	+	−	+
35	−	+	−	−	+	+	−	+	+	+	−	−	−	−	−	−	+	+	+	−	+	+	+	+	+
20	−	−	+	+	+	−	+	+	+	+	+	−	−	−	+	+	−	+	−	−	+	−	−	+	+
8	−	−	+	+	+	−	+	−	+	+	−	−	+	+	+	−	+	−	−	−	−	+	−	−	+
34	+	−	−	+	+	−	+	−	+	−	−	−	−	+	−	+	+	+	−	+	+	+	+	+	−
24	−	−	−	+	−	−	+	+	+	−	+	+	+	+	−	−	−	+	+	+	−	+	−	−	+
13	+	+	+	+	−	−	−	+	+	+	−	+	−	−	−	−	+	+	−	+	−	+	−	−	−
15	−	+	+	+	+	+	−	−	+	+	+	+	−	+	−	+	−	−	+	+	−	+	−	+	−
7	−	+	+	+	−	+	−	−	+	−	−	+	+	−	−	+	−	−	−	−	+	−	−	+	+
33	−	−	+	+	−	+	−	+	+	−	−	−	+	−	+	+	+	−	+	+	+	+	+	−	−
36	−	−	−	−	−	−	−	−	+	−	−	−	−	−	−	−	−	−	−	−	−	−	−	−	−
28	+	−	+	−	−	−	−	+	+	−	+	+	+	−	+	+	+	+	−	−	−	+	+	+	−
22	−	+	−	−	+	+	+	−	+	+	+	+	+	−	−	+	+	+	−	+	−	−	+	−	−
11	+	+	−	−	−	+	+	+	+	+	−	−	+	−	+	+	−	+	−	+	−	−	−	−	+
17	+	+	−	+	+	+	+	+	+	−	−	+	+	+	+	−	−	+	−	−	+	+	−	+	−
14	+	+	+	+	+	−	−	−	+	+	+	−	+	−	+	−	−	+	+	−	+	−	+	−	−

[a]In the table, "+" indicates high level and "−" indicates low level.

way to enhance heavy oil recovery is to improve the sweep efficiency.

Group 22 measures the adsorption capacity of reservoir rocks. Polymer loss due to adsorption can greatly affect the viscosity of polymer solution.

Group 16 represents the mobility reduction capability of polymer solution during the displacement. When polymer solution is injected into porous media, part of the polymer will be adsorbed on the surface of pores and the stretched long polymer molecular chains will hamper the flow of water and have no effect on oil flow. In waterflooding of heavy oils, water will break through quickly (e.g., see water cut in Figure 5) and the succeeding injected water tends to flow through the water channels because of smaller flow resistance. Polymer solution can more or less shut off this preferable flowing path and divert injected fluids to other zones of the porous medium, thus increasing the sweep efficiency and heavy oil recovery.

6.2.2. Secondary Scaling Groups. Group 8 represents the ratio of oil density to water density and can be also explained as the inertial force ratio.[38] However, the inertial force is incomparable to the viscous force in the displacement of heavy oils.

Group 9 represents the ratio between the gravity force and the viscous pressure drop. It has a minor effect on heavy oil recovery by polymer flooding. The reason is that the gravity force is usually quite small compared to the viscous force due to the high viscosity of heavy oils. Thus the effect of group 9 on heavy oil recovery by polymer flooding is negligible.

The dip angle group D_{10} has little effect on recovery. In both the experiments and numerical simulations, the polymer solution

dx.doi.org/10.1021/ie300328y | Ind. Eng. Chem. Res. 2013, 52, 911−921

was injected from the injection well at a constant rate so the dip angle does not influence the oil recovery rate. In addition, the dip angle will not cause evident gravity segregation since the density difference between water and heavy oil is small.[39] Therefore, the dip angle only has a negligible effect on heavy oil recovery by polymer flooding.

It was determined by sensitivity analysis that the ratio of capillary force to viscous force D_{12} has a limited effect on heavy oil recovery. This further supports the idea that the most effective way to enhance heavy oil recovery is to improve the volumetric sweep efficiency.

Groups D_1, D_2, D_5, D_6, D_{14}, D_{17}, D_{18}, D_{19}, D_{20}, D_{21}, and D_{23} were also determined to be secondary scaling groups according to sensitivity analysis.

All these secondary scaling groups can be relaxed during the scale-up of polymer flooding for heavy oil reservoirs.

7. CONCLUSIONS

1. Based on the 2-D polymer flooding model, a total of 26 dimensionless scaling groups were determined using inspectional analysis. Combining the scaling groups for heterogeneity, there are a total of 28 scaling groups for polymer flooding in heavy oil reservoirs.

2. By conducting simulation runs, the effectiveness of each of the 28 scaling groups was validated. For different combinations of parameters leading to the same numerical value of a certain scaling group, the effects on oil recovery were observed to be identical.

3. A sensitivity study identified nine dominant scaling groups as having significant effects on polymer flooding for enhanced heavy oil recovery. These dominant groups can be used as scaling criteria to design scaled laboratory experiments and to predict field-scale heavy oil recovery by polymer flooding.

APPENDIX

Table 7 shows the combinations of the group levels to be used in each run according to the Plackett−Burman design.

ASSOCIATED CONTENT

Supporting Information

Derivation of scaling groups for polymer flooding, including for initial and extended waterflooding and linear dependence between scaling groups. This material is available free of charge via the Internet at http://pubs.acs.org.

AUTHOR INFORMATION

Corresponding Author

*Tel.: (403) 210-7642. Fax: (403) 284-4852. E-mail: mingzhe.dong@ucalgary.ca.

Notes

The authors declare no competing financial interest.

ACKNOWLEDGMENTS

The financial support of the Petroleum Technology Research Center (PTRC) and Natural Sciences and Engineering Reservoir Council of Canada (NSERC) is gratefully acknowledged.

NOMENCLATURE

Variables

A_{p1}, A_{p2}, A_{p3} = parameters used for calculating polymer viscosity, $(\text{wt }\%)^{-1}$, $(\text{wt }\%)^{-2}$, $(\text{wt }\%)^{-3}$

b = parameter that controls the curvature the polymer adsorption isotherm, $(\text{wt }\%)^{-1}$

b_{rk}, c_{rk} = coefficients that describe permeability reduction effect, $(\text{wt }\%)^{-1}$

C_{ad} = polymer adsorption concentration, g/g

$C_{ad,max}$ = maximum polymer adsorption concentration, g/g

C_{pa} = polymer concentration, ppm

C_{pa}^{i} = concentration of injected polymer solution, ppm

C_{SEP} = effective salinity, ppm

D_i = ith scaling group, dimensionless

g = gravity acceleration, m/s^2

H = model dimension in the z-direction, m

$\overline{k}$ = average permeability, μm^2

k_x = permeability in the x-direction, μm^2

k_z = permeability in the z-direction, μm^2

k_{ra}^0 = end point relative permeability of aqueous phase, dimensionless

k_{ro}^0 = end point relative permeability of oleic phase, dimensionless

L = model dimension in the x-direction, m

n_a, n_o = relative permeability exponent for aqueous and oleic phases, dimensionless

p_a = aqueous phase pressure, kPa

p_c = capillary pressure, kPa

p_{ce} = entry capillary pressure of the rock sample, kPa

p_{wf} = well flowing pressure at $(x, z) = (L, H)$, kPa

p_o = oleic phase pressure, kPa

PV_p = slug size of polymer flooding, PV

PV_{w1} = slug size of preceded waterflooding, PV

PV_{w2} = slug size of extended waterflooding, PV

p_α = empirical coefficient that describes the shear thinning effect, dimensionless

q = flow rate, m^3/day

$R_{k,max}$ = maximum permeability reduction factor for water phase, dimensionless

S_a = saturation of the whole aqueous phase, dimensionless

S_{na}, S_{no} = normalized saturation for aqueous phase and oleic phase, dimensionless

S_p = slope, ppm^{-1}

S_o = saturation of oleic phase, dimensionless

S_{or} = residual oil saturation, dimensionless

S_{wi} = initial water saturation, dimensionless

S_{wr} = irreducible water saturation, dimensionless

V_{ax}, V_{az} = Darcy velocity of aqueous phase in x-direction and z-direction, m/s

V_{ox},V_{oz} = Darcy velocity of oleic phase in x-direction and z-direction, m/s

V_{DP} = Dykstra−Parson coefficient

V_T = total velocity, m/s

w_i = weight factor, dimensionless

Greek Symbols

ρ_o = oil density, kg/m^3

ρ_w = water density, kg/m^3

ρ_{avg} = average density, kg/m^3

α = dip angle, deg

ϕ = rock total porosity, dimensionless

ϕ_{IPV} = inaccessible porosity, dimensionless

μ_p = viscosity of polymer solution under zero shear rate, mPa·s

μ_p^0 = viscosity of polymer solution under zero shear rate, mPa·s

μ_o = oil viscosity, mPa·s

μ_w = water viscosity, mPa·s

γ = shear rate, s^{-1}

$\gamma_{1/2}$ = shear rate at which viscosity is the average of μ_p^0 and μ_w, s^{-1}

λ_i = pore size distribution index, dimensionless
λ_L = dimensionless correlation length

REFERENCES

(1) Alvarado, V.; Manrique, E. Enhanced Oil Recovery: An Update Review. *Energies* **2010**, *3* (9), 1529−157.
(2) Fairfield, W. H.; White, P. D. Lloydminster fireflood performance, modifications promise good recoveries. *Oil Gas J.* **1982**, *80* (6), 101−102.
(3) Wassmuth, F. R.; Green, K.; Hodgins, L.; Turta, A. T. Polymer flood technology for heavy oil recovery. Presented at the Petroleum Society's 8th Canadian International Petroleum Conference, Calgary, Canada, June 12−14, 2007; Paper 2007-182.
(4) Wang, J.; Dong, M. A laboratory study of polymer flooding for improving heavy oil recovery. Presented at the Petroleum Society's 8th Canadian International Petroleum Conference, Calgary, Canada, June 12−14, 2007; Paper 2007-178.
(5) Wang, J.; Dong, M. Optimum effective viscosity of polymer solution for improving heavy oil recovery. *J. Pet. Sci. Eng.* **2009**, *67*, 155−158.
(6) Patterson, G. Modeling and scale-up of mixing- and temperature-sensitive chemical reactions. *Ind. Eng. Chem. Res.* **2005**, *44* (14), 5325−5341.
(7) Groen, J. C.; Moulijn, J. A.; Pérez-Ramírez, J. Alkaline posttreatment of MFI zeolites. from accelerated screening to scale-up. *Ind. Eng. Chem. Res.* **2007**, *46* (12), 4193−4201.
(8) Sedov, L. I. *Similarity and Dimensional Analysis in Mechanics*; Academic Press: New York, 1959.
(9) Flandro, G. A.; Mcmahon, H. M.; Roach, R. L. *Basic Aerodynamics: Incompressible Flow*; Cambridge University Press: Cambridge, U.K., 2011.
(10) Ruark, A. E. Inspectional analysis: a method which supplements dimensional analysis. *J. Elisha Mitchell Sci. Soc.* **1935**, *51*, 127−132.
(11) Buckingham, E. On physically similar systems: illustrations of the use of dimensional equations. *Phys. Rev.* **1914**, *4*, 345−376.
(12) Peters, E. J.; Afzal, N.; Gharbi, R. On scaling immiscible displacements in permeable media. *J. Pet. Sci. Eng.* **1993**, *9*, 183−205.
(13) Rapoport, L. A. Scaling laws for use in design and operation of water-oil flow model. *Trans. AIME* **1955**, *204*, 143−150.
(14) Van Daalen, F.; Van Domselaar, H. R. Scaled fluid-flow models with geometry differing from that of prototype. *Soc. Pet. Eng. J.* **1972**, *12*, 220−228.
(15) Thomas, S.; Ali, F.; Thomas, N. H. Scale-up methods for micellar flooding and their verification. *J. Can. Pet. Technol.* **2000**, *39* (4), 18−27.
(16) Gharbi, R.; Peters, E.; Elkamel, A. Scaling miscible fluid displacements in porous media. *Energy Fuels* **1998**, *12*, 801−811.
(17) Gharbi, R. Dimensionally scaled miscible displacements in heterogeneous permeable media. *Transp. Porous Media* **2002**, *48*, 271−290.
(18) Algharaib, M.; Gharbi, R.; Malallah, A. Scaling immiscible displacement in porous media with horizontal wells. *Transp. Porous Media* **2006**, *65*, 89−105.
(19) Jin, L.; Wojtanowicz, A. K.; Afonja, G.; Li, W. Scaling analysis of wells with downhole water loop completion for bottomwater control. *J. Can. Pet. Technol.* **2010**, *49* (11), 81−90.
(20) Zendehboudi, S.; Chatzis, I.; Mohsenipour, A. A.; Elkamel, A. Dimensional analysis and scale-up of immiscible two-phase flow displacement in fractured porous media under controlled gravity drainage. *Energy Fuels* **2011**, *25*, 1731−1750.
(21) Islam, M. R.; Farouq Ali, S. M. New scaling criteria for polymer emulsion and foam flooding experiments. *J. Can. Pet. Technol.* **1989**, *28* (4), 79−87.
(22) Rai, K. Screening Model for Surfactant-Polymer Flooding Using Dimensionless Groups. M.S. Thesis, University of Texas at Austin, Austin, 2008.
(23) Brooks, R. H.; Corey, A. T. Properties of porous media affecting fluid flow. *J. Irrig. Drain. Div., Am. Soc. Civ. Eng.* **1966**, *92* (2), 61−90.
(24) Flory, P. J. *Principles of Polymer Chemistry*; Cornell University Press: New York, 1953.
(25) Meter, D. M.; Bird, R. B. Tube flow of non-Newtonian polymer solutions: Part I. Laminar flow and rheological models. *AIChE J.* **1964**, *10*, 878−881. Meter, D. M. Tube flow of non-Newtonian polymer solutions: Part II. Turbulent flow. *AIChE J.* **1964**, *10*, 881−884.
(26) Lin, E. A Study of Micellar/Polymer Flooding Using a Compositional Simulator. Dissertation, University of Texas at Austin, Austin, 1981.
(27) Wreath, D.; Pope, G. A.; Sepehrnoori, K. S. Dependence of polymer apparent viscosity on the permeable media and flow conditions. *In Situ* **1990**, *14* (3), 263−284.
(28) Larry, W. L. *Enhanced Oil Recovery*; Prentice Hall: Englewood Cliffs, NJ, 1989.
(29) Center for Petroleum and Geosystems Engineering. *Technical Documentation for UTCHEM-9.0, A Three-Dimensional Chemical Flood Simulator*; The University of Texas at Austin, Austin, TX, 2000; Vol. II.
(30) Shook, M.; Lake, L. W.; Li, D. Scaling immiscible flow through permeable media by inspectional analysis. *In Situ* **1992**, *16* (4), 311−349.
(31) Akram, F. A better understanding of heavy oil reservoir. *Digital Energy J.* **2012**, *35*, 22−23.
(32) Deutsch, C. V.; Journel, A. G. *GSLIB Geostatistical Software Library and Users Guide*; Oxford University Press: New York, 1992.
(33) Waggoner, J. R.; Castillo, J. L.; Lake, L. W. Simulation of EOR processes in stochastically generated permeable media. *SPE Form. Eval.* **1992**, *7*, 173−180.
(34) Lambert, M. E. A Statistical Study of Reservoir Heterogeneity. M.S. Thesis, University of Texas at Austin, Austin, 1981.
(35) Jensen, J. L.; Lake, L. W.; Corbett, P. W. M.; Goggin, D. J. *Statistics for Petroleum Engineers and Geoscientists*; Prentice Hall: Englewood Cliffs, NJ, 1997.
(36) Plackett, R. L.; Burman, J. P. The design of optimum multifactorial experiments. *Biometrika* **1946**, *33* (4), 305−325.
(37) Ryan, B. F.; Joiner, B. L.; Cryer, J. D. *MINITAB Handbook: Updated for Release 16*; Brooks/Cole: Independence, KY, 2012.
(38) Bai, Y.; Li, J.; Zhou, J. Effects of physical parameter range on dimensionless variable sensitivity in water flooding reservoirs. *Acta Mech. Sin.* **2006**, *22*, 385−391.
(39) Arhuoma, M.; Dong, M.; Yang, D.; Idem, R. Determination of water-in-oil emulsion viscosity in porous media. *Ind. Eng. Chem. Res.* **2009**, *48*, 7092−7102.